

Publication

(submitted)

A specific structure within the *Alu* domain of the Signal Recognition Particle RNA Is Important for Elongation Arrest Activity

Laurent Huck¹, Monique Fornallaz¹, Yves Thomas^{1,5}, Arthur E. Johnson², Harris D. Bernstein³, Oliver Weichenrieder^{4,6}, Steven Cusack⁴ and Katharina Strub^{1,7}.

¹) Département de Biologie Cellulaire
Université de Genève
CH-1211 Genève 4, Switzerland

²) Texas A&M University, Health Science Centre
College of Medicine
College Station, TX-77843-1114, USA

³) Genetics and Biochemistry Branch,
National Institute of Diabetes and Digestive and Kidney Diseases,
National Institute of Health
10, Centre Drive
Bethesda 20892-1810, Maryland, USA

⁴) European Molecular Biology Laboratory, Grenoble Outstation
6, Rue Jules Horowitz
F-38042 Grenoble, CEDEX 9, France

⁵) Current address: Centre National de l'Influenza
Laboratoire Central de Virologie
Hôpital Cantonal Universitaire
24, Rue Micheli-Du-Crest
1211 Genève 14

⁶) Current address: Dept. of Molecular Carcinogenesis - H2
The Netherlands Cancer Institute
Plesmanlaan 121
1066 CX Amsterdam, Netherlands

⁷) Corresponding author:

Telephone: +41-22-702-6724

Fax: +41-22-702-6644

Email : Strub@cellbio.unige.ch

ABSTRACT

The eukaryotic signal recognition particle (SRP) tightly links protein synthesis to translocation into the endoplasmic reticulum (ER) by delaying elongation of the nascent chain during co-translational targeting. The results presented here provide evidence that a specific RNA structure in the *Alu* domain of SRP plays an important role in the elongation arrest activity of SRP. Three base pairs between two distant loops, L2 and L1.2, form an extended stack together with an additional base from each loop. Mutations in L2 that disrupt base pairing diminished the elongation arrest activities of reconstituted SRPs. Complementary mutations in L1.2 fully restored elongation arrest activities despite the differences in the primary sequences of the loops. Mutations in L1.2 had less dramatic effects on the function of SRP. Hence, the well-defined, rigid structure of loop L2 appears to play a fundamental role in the formation and the stability of the tertiary structure. The loss in elongation arrest activity is not explained by the absence of h9/14 in the particles or by another assembly defect. Instead, it is an intrinsic property of SRPs containing RNAs with mutations that impair formation of the tertiary structure. A structure-based alignment reveals a significant conservation of the structural elements that may allow formation of the tertiary structure, a result that underlines the importance of the tertiary structure in SRP function.

INTRODUCTION

The signal recognition particle (SRP) plays an essential role in targeting proteins to the endoplasmic reticulum (ER, review see (1)), which is the first step in routing proteins into the secretory pathway. SRP samples translating ribosomes for nascent chains bearing signal sequences, a common hallmark of ER-targeted proteins. Signal sequence recognition results in an arrest or a delay in polypeptide elongation. An interaction of SRP with its receptor (SR) in the ER membrane targets the SRP-ribosome-nascent chain complex to the translocon, a specific structure in the membrane that promotes translocation into the ER (for review see (2,3)). At the translocon, translation resumes at its normal speed and the nascent chain is transferred across or into the ER membrane while the released SRP enters a new targeting cycle. Three GTPases control the targeting process: The signal sequence binding protein SRP54 and the two subunits of SR, SR α and SR β (for review see (4)). In this model, SRP serves as an adaptor between protein synthesis and the translocation process into the ER.

SRP can bind to all ribosomes and its affinity increases in the presence of an exposed signal sequence (5,6). Notably, SRP can distinguish between actively translating and inactive ribosomes and therefore appears to recognise conformational changes in the ribosome (7). This notion is also supported by the observation that SRP interacts with the ribosome at a specific stage in the elongation cycle, just before peptidyl-tRNA undergoes translocation from the A site to the P site (8). Furthermore, SRP interacts with the ribosome to delay elongation of the nascent chain upon signal sequence recognition, which is referred to as the elongation arrest activity (9,10). It is thought to prevent premature folding of the nascent chain, which may interfere with efficient translocation. In yeast, abrogating elongation arrest activity impairs the tight coupling of translation and translocation, although a significant translocation defect could not be observed for several proteins (11).

The signal recognition and targeting functions of mammalian SRP are contained within the S domain, which comprises the central part of SRP RNA and the proteins SRP19, SRP54 and SRP68/72 (6,12). The signal sequence binding protein SRP54 could be cross-linked to two ribosomal proteins in the vicinity of the nascent chain exit site (13). Similarly, cross-links between bacterial SRP and ribosomes are also consistent with its location close the nascent chain exit site (14,15). The *Alu* domain, which comprises the 3' and 5' ends of SRP RNA and the SRP9/14 heterodimer, is required for the elongation arrest activity of SRP as deduced from the observation that the S domain alone lacked this activity (16). However, the S domain alone also lacks signal sequence-independent ribosome binding activity (17). A small C-terminal truncation of SRP14 specifically abrogated the elongation arrest of the particle without interfering with signal sequence recognition or ribosome-binding (18) indicating that direct interactions between the *Alu* domain and the ribosome may indeed mediate the arrest or delay in nascent chain elongation.

In recent years, significant progress has been made in determining the structure of SRP (for review see (19)). The *Alu* portion of SRP RNA includes a 5' domain comprising two hairpin structures linked by a conserved single-stranded region and a short stem as well as a 3' domain including a portion of the central stem connecting the *Alu* and the S domains (Fig. 1). The crystal structure of the *Alu* RNA 5' domain bound to SRP9/14 revealed that it is compactly folded into two helical stacks, which are connected by the single-stranded region forming a U-turn (20). In agreement with previous footprinting studies (21), the U-turn and adjacent nucleotides represent the primary binding site of the SRP9/14 heterodimer. Opposite the protein-binding site, the two loops of the 5' domain form three base pairs (20). Formation of this tertiary structure is most likely induced and/or stabilised upon protein binding (22). The potential to form base pairs between the two distant loops is conserved in SRP RNAs of *Metazoa* and of *Archaea* as well as of the bacterial species *Bacillus* and *Clostridium* (23,24).

Further biochemical and structural data support a model in which the complete *Alu* domain may exist in two conformations (25). In the open conformation, the central stem would not participate in complex formation with SRP9/14 whereas in the closed conformation, the central stem would fold back by up to 180° to align beside the 5' domain allowing contacts to the SRP9 moiety of the protein. The model for the closed conformation is consistent with the observed footprints on the central stem (21) and with the requirement that the 3' and the 5' domains have to be flexibly linked for fully efficient binding of SRP9/14 (26).

The RNA moieties of ribonucleoprotein complexes are known to play essential roles in many diverse cellular processes. By analogy, SRP RNA may play an active role in the specific targeting process rather than just serving as a scaffold for the proteins. In particular, the conservation of the RNA moiety in the *E. coli* SRP, which contains just one protein subunit, argues strongly against a scaffold role of SRP RNA. So far, a specific role of the RNA has been characterized in the interaction between SRP and its receptor. It accelerates complex formation between the two, which leads to an increase in the observed GTP hydrolysis rate (27-29). Additional observations also support a functional role of the RNA. In the *E. coli* particle, the RNA stabilises the structure of the signal sequence recognition protein (Ffh, (30)). Conformational changes in the RNA upon binding of SRP to polysomes (22), suggest a role for SRP RNA in the interaction with the ribosome and conformational changes in one of the loops of the 5' *Alu* domain were associated with a loss of elongation arrest function of the particle (18). Particularly interesting is the finding that trypanosome SRP comprises two RNA species: SRP RNA, which has a truncated 5' domain structure, and a tRNA-like RNA (sRNA-85) linked to the 5' domain of SRP RNA (31,32). It is hard to explain the acquisition of sRNA-85 without evoking a significant role of the RNA.

The tertiary RNA structure formed between the two loops in the *Alu* domain of SRP RNA is not bound by the protein and is therefore presumably free to interact with other cellular components such as the ribosome. This structure was therefore an interesting putative candidate for a functional role of SRP RNA in elongation arrest activity. To examine this hypothesis, we produced synthetic SRP RNAs with individual mutations in both loops that would disrupt base pairing, and with simultaneous mutations in both loops that would restore base pairing with a different primary sequence. The mutated RNAs were reconstituted into SRP and assayed for their elongation and translocation activities. We report here that the tertiary structure formed between the two distant loops is required for elongation arrest activity. Mutations disrupting the tertiary structure reduced the elongation arrest activity of reconstituted SRP. The loss of elongation arrest activity was the direct result of changing the RNA structure and was not due to the absence of h9/14 or another assembly defect. The functional importance of the structure is emphasised by its significant conservation.

MATERIALS AND METHODS

Mutated SRP RNA and *Alu* RNA genes

Mutations at specific sites in the SRP RNA gene were introduced by polymerase chain reaction (PCR) using the QuickchangeTM method (Stratagene). The primer oligonucleotides contained the desired mutations flanked by 15 nucleotides (Interactiva, Germany). As template for the polymerase chain reaction, we used either the plasmids p7Swt (21) or pSA86H (26). Clones with complementary mutations in two different regions were obtained in two steps. All clones were verified by automatic sequencing. Nomenclature for the mutated SRP RNAs: The first number indicates the mutated nucleotides followed by the name of the loop. For example 2L2 represents the mutation of two nucleotides in L2.

RNA synthesis

Plasmids were linearized with Xba I (Gibco BRL) before synthesis of the RNA with T7 RNA polymerase in 100 μ l reactions (40 mM Tris-HCl pH 8.1, 20 mM MgCl₂, 1 mM spermidine, 5 mM dithiothreitol (DTT), 4 mM of each rNTPs, 1 μ g/ μ l BSA, 100 ng/ μ l DNA template and 22 U/ μ l T7 RNA polymerase. The plasmid for expression of T7 RNA polymerase was the kind gift of (33). Nucleotides were obtained from Sigma and stored as 50 mM solutions at -80°C. After transcription, the DNA was digested with RQ1 RNase-free DNase (Promega), the samples extracted with phenol and purified on a 1 ml Sephadex G50 (fine, Pharmacia) column. The RNAs were precipitated and dissolved in sterile water. The qualities and the quantities of the RNAs were verified on denaturing polyacrylamide gels and by measuring the optical density at 260 nm. For the synthesis of radiolabelled RNA, we used α [³²P] UTP (24.10⁵ Bq/mmol, Amersham Biosciences).

SRP proteins

The proteins h9, h14 and h ϕ 19 were expressed in *E. coli* from the plasmid pEh9, pEh14 and pE ϕ 19 (18,34) using the T7 RNA polymerase expression system (35). Cells were lysed in a French PressTM and the extracts of h9 and h14 were combined for purification. The h9/14 heterodimer was purified by Hi-Trap Heparin (Amersham Biosciences), by hydroxylapatite (BioRad) and by Superdex-200 (Amersham Biosciences) chromatography. The protein h ϕ 19 was purified by Hi-Trap Heparin, CM and Superdex-200 (Amersham Biosciences) chromatography. Canine SRP54 was expressed in the baculovirus system (6). SF21 cells were used to amplify the virus encoding for SRP54, whereas the protein was produced in Tn5 cells. Following lysis of the cells in a homogenizer, the protein was purified on a CM and on Hi-Trap Heparin column (Amersham, Pharmacia, Biotech). The purified proteins were quantified by spectrophotometry at 280 nm. Molar extinction coefficient $\epsilon_{h9/14}$: 15 130 M⁻¹ cm⁻¹, $\epsilon_{h\phi 19}$: 12 570 M⁻¹ cm⁻¹ and ϵ_{54} : 22 220 M⁻¹ cm⁻¹. Canine SRP68/72 was purified from canine SRP as described in (12).

Elongation arrest and translocation assays

SRP was reconstituted with SRP RNA, canine SRP68/72 and recombinant SRP9/14, SRP19 and SRP54 proteins. Reconstitutions were done in 8 μ l at 0.5 μ M and 1 μ M final concentrations of all the proteins and *in vitro* transcribed SRP RNA, respectively, in 20 mM HEPES-KOH, pH 7.5, 500 mM potassium acetate (KOAc), pH 7.5, 5 mM magnesium acetate (MgOAc), 0.01% (v/v) Nikkol, 1 mM DTT. Samples were incubated for 10 minutes on ice and for 10 minutes at 37°C. Reconstituted SRP was then added at the desired concentrations to 10 μ l wheat germ translation reactions, programmed with synthetic preprolactin and sea urchin cyclin D transcripts as described in (36). Translation reactions were stopped after 30 minutes at 26°C, proteins precipitated with 10% (w/v) trichloroacetic acid and analysed by 12% SDS-PAGE. Preprolactin, prolactin and cyclin D were quantified by the use of a phosphorescence imaging system (BioRad). To monitor translocation, the 10 μ l wheat germ

translation reactions were complemented with SRP-depleted canine microsomes (0.15 eq./ μ l) prepared as described in (37). Elongation arrest and translocation efficiencies were evaluated as follows:

$$EA = [1 - \frac{Ps/Cs}{Po/Co}] \times 100$$

where EA is percent elongation arrest activity, Ps and Cs are the amounts of

preprolactin and cyclin quantified in the sample and Po and Co the amounts of preprolactin and cyclin present in the negative control (SRP buffer or SRP reconstituted without h9/14).

$T = 100 \times [P / (pP + P)]$ where T is percent translocation, P is the amount of prolactin and pP the amount of preprolactin quantified in each sample. T is about 20% without the addition of purified canine SRP or reconstituted particles. All SRPs were tested in at least two independent experiments. For purification by ion exchange chromatography, SRP was reconstituted in 50 μ l reactions at final concentrations of 2 μ M of each protein and 12 μ M of synthetic SRP RNA in 50 mM HEPES-KOH, pH 7.5, 500 mM KOAc, pH 7.5, 5.5 mM MgOAc, 0.01% (v/v) Nikkol, 1 mM DTT, 0.5 mM EDTA, pH 7.5, 10% (v/v) glycerol. Fully reconstituted particles were purified away from incomplete particles through a 50 μ l DE53 column essentially as described in (38). Samples were eluted twice with 50 μ l 50 mM HEPES-KOH, pH 7.5, 600 mM KOAc, pH 7.5, 6.5 mM MgOAc, 0.01% (v/v) Nikkol, 1 mM DTT, 0.5 mM EDTA, pH 7.5, 10% (v/v) glycerol and twice with 50 μ l of the same buffer containing 1000 mM KOAc and 10 mM MgOAc. Aliquots of all fractions were precipitated with 10% (w/v) trichloroacetic acid and analysed by 5-20% SDS-PAGE followed by silver staining. Complete particles eluted at 600 mM KOAc, whereas incompletely reconstituted particles eluted at 1000 mM KOAc. The concentrations of the purified particles were first evaluated by silver staining. However, for greater accuracy we quantified the SRP samples by Western blot analysis using affinity-purified antibodies against SRP14 and SRP54.

RNA binding assays

The protein h14 was synthesised in 10 μ l wheat germ translation reactions in the presence of 1 pmole of recombinant h9 (34). The heterodimer h9/14 was bound to 2 pmole of biotinylated SRP RNAs in 50 mM HEPES-KOH, pH 7.5, 350 mM KOAc, pH 7.5, 3.5 mM MgOAc and 0.01% (v/v) Nikkol. The bound protein was purified away from unbound protein by the use of magnetic Streptavidin beads (Dyna) as described in (39). Bound proteins were analysed by 15% SDS-PAGE, visualised by autoradiography and quantified with the phosphoimager (BioRad).

Electromobility shift assays

To set up the conditions for the competition experiments, 200 nM cold SA86 RNA (containing 20 000 cpm of labelled SA86 RNA as a tracer) was titrated against h9/14 at concentrations ranging from 25-600 nM. Conditions allowing optimal complex formation in the absence of an excess of protein were achieved at 190 nM h9/14. Individual reconstitution assays were done in 20 mM Hepes pH 7.5, 300 mM KOAc, 10 mM MgOAc, 5 mM DTT, 0.015% (v/v) Nikkol. For reconstitution, 5 μ l of RNA pSA86 (containing 20 000 cpm of labelled RNA) were recombined with 5 μ l of competitor RNA and 10 μ l of h9/14. The binding reactions were allowed to proceed for 10 minutes on ice, then for 10 minutes at 37°C. Labelled and unlabelled RNAs were annealed in assay buffer without DTT and Nikkol immediately before use. The final concentrations of competitor RNAs ranged from 50 to 800 nM. Negative control samples consisted of SA86 RNA alone and in the presence of equivalent amounts of bovine serum albumin. Native 8% polyacrylamide gels (acrylamide/bisacrylamide 40:1) containing 10 mM MgOAc and 50 mM Tris acetate pH 7.5 were prerun at 0.22 W/cm³ for two hours in the cold room. Reconstitution samples in buffers without dye were mixed with 4 μ l 80% (v/v) glycerol prior to loading and were run for 120 minutes at 0.22 W/cm³ in the cold room. Gels were then fixed with 20% (v/v) methanol, 10% (v/v) acetic acid for 30 minutes and dried before autoradiography or exposure to phosphoimager screen. Relative dissociation constants were calculated as described

(34) using the following equation: $\frac{Kdwt}{Kdcomp} = \frac{[Rwt]}{[RwtP]} \times \frac{[RcompP]}{[Rcomp]}$ (1) where [R] represents free

RNA, [P] free protein and [RP] the complex. Taking into consideration that

$[R_{comp}P] = (v_0 - v) \times [R_{wt}]; [R_{wt}P] = v \times [R_{wt}]; [R_{comp}] = [R_{ocomp}] - (v_0 - v) \times [R_{wt}]$
and $[R_{wt}] = [R_{wt}] - v \times [R_{wt}]$, equation 1 can be transformed into

$$\frac{[R_{ocomp}]}{(v_0 - v) \times [R_{wt}]} - 1 = \frac{K_{dcomp}}{K_{dwt}} \times \left(\frac{1}{v} - 1\right) \quad (2)$$

where v_0 and v represent fractions of the wt RNA bound to the protein in the absence and in the presence of different competitor concentrations, respectively. $[R_{wt}]$ and $[R_{ocomp}]$ are the concentrations of wild type and competitor RNA, respectively, used in the experiments. The slope represents the ratio between the dissociation constants of the competitor and SA86 RNA.

Computer programs and data bases

For the sequence comparison of SRP RNAs we used the SRP database by (23) (<http://www.psych.uthct.edu/dbs/SRPDB/SRPDB.html>). The image of the *Alu* RNP structure were generated as povscript file with the Swiss PDB viewer and rendered by Pov-Ray™.

RESULTS

SRP RNA mutagenesis and SRP9/14 binding

The 5' domain of *Alu* RNA is folded into a compact structure consisting of two helical stacks connected by a U-turn, which determines the relative orientation of the stacks (Fig. 1A and B, H1.1, H1.2 and H2; (20)). The single-stranded U-turn motif is highly conserved in primary sequence and represents the major protein-binding site. However, the protein makes additional contacts to the central stem (3' domain), which is thought to flip back by almost 180° to align alongside the compactly folded 5' domain (Fig. 1B). The RNA-protein complex is further stabilised by tertiary RNA contacts between helix H2 and the central stem and a tertiary structure consisting of three G-C base pairs, which are formed between the two distant loops L1.2 and L2 (Fig. 1, G13-C37, G14-C34 and C15-G33). Whereas loop L2 is very rigid as it is constrained by a U-turn at position U12 and by a sheared G11-G16 base pair (Fig. 1), loop L1.2 is rather flexible lacking internal stabilizing structures. Another striking feature of the tertiary structure is the stack formed by the three base pairs and which is extended on both sides with purines from either loop L2 or loop L1.2 (Fig. 1, G16 and A36).

To assess the role of the tertiary base pairs in elongation arrest activity of SRP, we specifically mutated two and three positions in each loop individually or in both loops simultaneously (Fig. 2A). Guanidine was replaced by cytidine and vice versa. Hence, the complementary mutations restored either two or three G-C base pairs. First, we studied whether the mutated SRP RNAs were still able to bind SRP9/14, since its presence is a prerequisite for elongation arrest activity of SRP (16). Binding of SRP9/14 was examined using biotinylated SRP RNAs and *in vitro* synthesised human SRP14 (h14) complemented with recombinant human SRP9 (h9). As previously observed (39), wild type SRP RNA bound 30% of the protein h9/14 used in the assay (Fig. 2B and C, compare Input and WT). Although some differences could be seen, all of the mutated SRP RNAs were able to bind h9/14 as compared to the negative control (lane 3). Mutations in loop L1.2 and two compensatory mutations in both loops had no effect on the binding efficiency, whereas three compensatory mutations in both loops increased the binding efficiency. Both SRP RNAs with mutations in loop L2 showed a two-fold decrease in the binding efficiency. Hence, changes in the primary sequences of the loops did not abolish protein binding, but moderately changed the binding efficiencies of h9/14. To examine whether the observed effects were the fortuitous results of the specific changes we made, we tested six other mutated RNAs in which G14,C15 and G33,C34 were changed into uridines and adenines (Fig. 2D). We observed similar results as with the previous mutations. RNAs with complementary mutations and the RNA with the mutation A33A34 in loop L1.2 bound h9/14 like wild type. The two RNAs with mutations in loop L2 were reduced to 41 and 44%, respectively. Notably, the double mutation in loop L1.2, U33U34, also had a slightly reduced binding efficiency (77%).

It has previously been observed that G13 and G14 can be modified in naked SRP RNA but not in SRP (22) suggesting that tertiary base pairing occurs upon protein binding. Hence, the three base pairs are likely to contribute to stabilising the RNA-protein complex and their disruption might therefore be expected to have a moderate impact on the efficiency of complex formation. Most importantly, the effects of the mutations in one loop were always rescued by complementary mutations in the other loop consistent with the interpretation that they were due to the disruption of base pairing and not due to the changes in the primary sequences *per se*. However, it remained puzzling that only mutations in L2 and not in L1.2 had noticeable effects on binding. It suggested that as long as the primary structure was conserved in L2, base pairing had only an auxiliary function for protein binding. However, when loop L2 is mutated, base pairing becomes essential to compensate the negative effects.

In order to determine whether the observed decrease in the efficiencies reflected a significant change in the dissociation constants of the complexes, we used a quantitative approach to study the effects of the mutations. We have previously compared dissociation constants of *Alu* RNA variants in competition experiments with an electrophoretic mobility shift assay (EMSA, (25)). Complete SRP RNA could not be used in these experiments, because free RNA and the RNA-protein complex were not separated sufficiently. We therefore made the 2L2, 2L1.2 and 2 Comp mutations in SA86 RNA,

which comprises all elements required for h9/14 binding (26). The relative dissociation constants were then determined with competition experiments (Materials and Methods) In addition, we also made a variation of the triple mutations made in complete SRP RNA. Instead of changing all three nucleotides in one loop, we mutated the three guanidines (G13G14G33) simultaneously into cytidines and the three cytidines (C15C34C37) into guanidines. Notably, the complementary mutation 3 Comp was identical in *Alu* SA86 RNA and complete SRP RNA. In these experiments, we used the same experimental conditions as described in (25) (see also Material and Methods). The results (Fig. 3 A and B) demonstrated that the dissociation constants of the various mutated SA86 RNAs differed very little from the dissociation constant of wild type *Alu* SA86 RNA. Consistent with the previous results, the biggest difference was seen with the 2L2A RNA with an apparent dissociation constant three-fold lower than wild type SA86 RNA. If this difference reflected a decreased kinetic stability of the complex, it might account for the lower binding efficiency in the RNA binding experiments. Although SA86 RNA comprises all elements required for high efficient binding of h9/14, we cannot entirely exclude the possibility that mutations in the complete SRP RNA have a stronger effect on h9/14-binding than the same mutations in *Alu* SA86 RNA.

In summary, we concluded from these results that certain nucleotide changes in the loops designed to interfere with base pairing moderately influenced the binding efficiency of h9/14. The effects were suppressed, if base pairing was restored. Importantly, taking into consideration that the *Alu* RNA-h9/14 complex is very stable (dissociation constant in the subnanomolar range (34,40), it was unlikely that the small changes observed would interfere with reconstituting SRP for functional assays.

Functional analysis of SRPs comprising mutated RNAs

SRP was reconstituted (41) from canine and recombinant SRP proteins together with synthetic SRP RNAs. The RNAs were produced in large-scale transcriptions and purified away from DNA and nucleotides under non-denaturing conditions. Human SRP19 (h19) and canine SRP54 were expressed in *E. coli* and insect cells, respectively. SRP68/72 was purified from canine SRP. The conditions for reconstituting SRP were optimised by testing different protein and RNA concentrations (results not shown). A slight excess of RNA over protein gave the highest yield in active particles (see below). Translocation and elongation arrest activities of the reconstituted particles were assayed in a wheat germ translation system. To examine their elongation arrest activities, we monitored the relative inhibition of preprolactin synthesis (a secreted protein) as compared to cyclin D synthesis (a cytoplasmic protein). To examine the signal recognition and targeting activities of the particles, we assayed their capacities to promote translocation into salt-washed canine microsomes as revealed by processing of preprolactin to prolactin (Material and Methods). Particles with intact signal recognition and targeting functions, but lacking elongation arrest activity, have their translocation capacities reduced by about 50% (12,18).

The positive controls, canine SRP and SRP reconstituted with canine RNA efficiently and specifically inhibited preprolactin synthesis as compared to cyclin synthesis at a final concentration of 100 nM (Fig. 4A, upper panel, lanes 2 and 3, 94% and 91% inhibition, respectively). The signal recognition and targeting activities of the same particles resulted in the processing of 85 and 81% of preprolactin to prolactin (lower panel, lanes 2 and 3). At the same concentration, the elongation arrest and processing activities of particles reconstituted with synthetic wild type RNA (WT RNA) were 78 and 43%, respectively (lane 4 upper and lower panel, respectively). No activities were detected at particle concentrations below 25 nM (results not shown). Hence, synthetic SRP RNA was less active in reconstituting functional particles. Re-annealing the RNA under different conditions as well as increasing the amount of RNA in the reconstitution reactions (see below) failed to improve the reconstitution efficiency.

In the following, we compared the elongation arrest and translocation activities of particles reconstituted with mutated SRP RNAs to the activities of particles reconstituted with synthetic WT RNA. Disrupting base pairing through mutations in loop L2, 2L2 and 3L2 RNAs, resulted in a significant loss of elongation arrest activity (Fig. 4A and B) whereas a moderate loss was observed

with three mutations in loop L1.2 (3L1.2 RNA). Two mutations in loop L1.2 had no significant effect on the elongation arrest activity of the particle. Most importantly, mutations in the complementary loop always rescued the negative effects of the first mutations confirming that the RNA tertiary structure and not the changes in the primary sequence caused the loss in elongation arrest activity. Interestingly, not all mutations appeared to affect elongation arrest activity to the same extent suggesting that they interfered to variable degrees with the formation of the tertiary structure. Mutations in loop L2 appeared to be more detrimental to elongation arrest activity than mutations in loop L1.2.

All SRPs containing mutated synthetic RNAs promoted translocation into salt-washed membranes and were therefore active in signal recognition and targeting (Fig. 4A and C). Hence, disrupting base pairing interfered predominantly with the elongation arrest function of SRP. In addition, the processing efficiencies were in agreement with the observed elongation arrest activities. All SRPs with defective elongation arrest functions had reduced translocation efficiencies as compared to WT SRP (Fig. 4, lanes 2L2, 3L2 and 3L1.2).

Defective elongation arrest activity is the intrinsic property of fully assembled mutated SRPs and not the result of an assembly defect.

We made several experiments to confirm that the observed decrease in elongation arrest activity was indeed an intrinsic property of SRPs comprising certain mutated SRP RNAs and was not due to incomplete assembly.

First, we examined whether increasing the amount of RNA in the reconstitution reaction improved elongation arrest activity. The reconstitution conditions have been elaborated with WT RNA and it was feasible that the mutated RNAs had a different activity in reconstituting active particles. SRP was reconstituted in the presence of a constant amount of all proteins and increasing concentrations of SRP RNAs. Binding of SRP proteins has previously been observed to be cooperative (41). An excess of RNA within certain concentration limits was therefore not expected to interfere with the assembly of fully reconstituted particles. In these experiments, we compared WT RNA to 3L2 RNA (Fig. 5A and B). Elongation arrest and translocation assays were performed as before. For WT RNA, reconstitutions worked best with an excess of 1.5-fold of RNA over protein (white bars). For 3L2 RNA maximal elongation arrest activity was observed at a four-fold excess of 3L2 RNA. Notably, the elongation arrest activity remained within the error bars around 35-45% inhibition as compared to WT SRP between a two-fold to eight-fold excess of RNA. All particles were still active in signal recognition and targeting as indicated by their processing activities. In addition, the observed processing efficiencies confirmed the results of the elongation arrest assays. The processing efficiencies were decreased for particles that had a partially defective elongation arrest function.

Second, we titrated h9/14 into reconstitution reactions with 3L2 and WT RNAs. The excess of protein was thought to ensure that h9/14 was driven into the RNA-bound state even after dilution into the translation reactions. In these experiments, the amounts of SRP RNA and of all proteins except h9/14 were kept constant in the reconstitution reactions whereas the amounts of h9/14 were increased to the extent indicated (Fig. 5C and D). As before, the 3L2 SRP had reduced elongation arrest and translocation activities as compared to WT SRP. Notably, both activities remained unchanged upon addition of up to an eight-fold excess of h9/14 indicating that the defect in the elongation arrest function was most likely not caused by the absence of h9/14 in the particle.

Third, we decided to purify the particles after reconstitution. This approach requires large amounts of native canine proteins. To complement the previous experiments, we therefore limited our analysis to the mutated particles 2L2, 2 Comp and, as a positive control, WT particles. The reconstitution reactions were purified by anion exchange chromatography to remove non-bound proteins and partially reconstituted particles (Materials and Methods). Fully assembled SRP is expected to elute at 600 mM potassium acetate (38,42). As predicted from the RNA-binding experiments 2L2 RNA bound all SRP proteins including h9/14 as visualised by silver staining (Fig. 6B, lane 2). WT and 2 Comp particles gave similar results (Fig. 6A, result not shown). Notably, SRP54 was the protein which bound with the lowest efficiency in all reconstitution reactions. The concentrations of the particles were determined by immunoblotting with anti-SRP14 and anti-SRP54

antibodies and by comparing to dilution series of recombinant h14 and canine SRP54 proteins (results not shown). The yield in purified SRP was about 30% of the protein input.

The purified particles were added at different concentrations into translation and translocation assays. At concentrations below 20 nM of purified SRP, none of the reconstituted particles exhibited a significant elongation arrest activity (Fig. 6C). As compared to the negative control, which contained buffer instead of SRP, we observed an apparently non specific inhibition of about 20% for all samples. We have previously observed the same level of non specific inhibition with a particle lacking the SRP9/14 protein (18). In addition, there were significant fluctuations in the ratio of preprolactin to cyclin in the absence of a specific effect on preprolactin synthesis as indicated by the large error bars. The error bars decreased noticeably as soon as elongation arrest activity could be detected. We can as yet not explain this observation. Corroborating our previous results, elongation arrest activity increased in a concentration-dependent manner upon addition of WT and 2 Comp SRPs. Particles with 2 Comp RNA were even more active than WT SRP, although the shift in the two curves might be enhanced by a slight error in the concentrations of the particles. In contrast, 2L2 particles had again a reduced elongation arrest activity. The apparently increased elongation arrest activity of 2L2 particles at a concentration of 40 nM was most likely the fortuitous result of the significant errors rates in the absence of elongation arrest activity. In contrast, preprolactin processing could be monitored more accurately for all samples and at low SRP concentrations. The results of the translocation assays supported the previous interpretation. The processing activity of 2L2 SRP increased more slowly than the ones of WT and 2 Comp SRPs as would be expected for an elongation arrest-defective particle (Fig. 6D). Notably, at concentrations around 40 nM both 2 Comp and WT SRPs reached maximal translocation activities. As previously observed, the translocation efficiency of 2L2 SRP was only half maximal at the same concentration. Interestingly, the translocation efficiency continued to increase at 80 nM 2L2 SRP and might ultimately reach the same level as WT SRP at sufficiently high concentrations of 2L2 SRP. Hence, the decrease in the translocation efficiency of an elongation arrest-defective SRP could be compensated with higher particle concentrations.

DISCUSSION

In these studies, we unravelled a function for a specific RNA structure in the *Alu* domain of SRP. It is directly required for elongation arrest activity and includes three tertiary base pairs between loop L2 and loop L1.2 that form an extended stack with one base from each loop. Mutations disrupting base pairing diminished elongation arrest activities of reconstituted SRPs, whereas complementary mutations in both loops fully restored elongation arrest activities to wild type levels despite the differences in the primary sequences of the loops. Mutations also had a moderate effect on protein binding. However, the loss in elongation arrest activity is not explained by the absence of h9/14 in the particles or by another assembly defect. It is an intrinsic property of SRPs comprising RNAs with mutations that impair formation of the tertiary structure.

The experimental strategy employed in these studies has previously been successfully exploited to prove functional roles of base pairing structures in many processes such as pre-mRNA splicing (43) and translation (44,45). In our experiments, we made the puzzling observation that individual mutations in loop L2 had stronger effects on elongation arrest activity of SRP and, to a much lesser extent, also on h9/14 binding, than mutations in loop L1.2. Or both mutations are expected to abolish base pairing between the loops. However, the negative effects of mutations in loop L2 were always completely rescued by complementary mutations in loop L1.2. Hence, if loop L2 remains unchanged, loop L1.2 mutations appear to have minor effects on *Alu* domain functions (see Fig. 4, lanes 2L1.2 and 3L1.2) whereas after mutation of loop L2, base pairing with loop L1.2 becomes essential for full elongation arrest activity (lanes 2L2 and 3L2). In structural terms, these results are consistent with the hypothesis that in addition to Watson-Crick base pairing *per se* an additional L2-specific factor may influence the formation and the stability of the tertiary structure.

As mentioned before, loop L2 has a highly ordered structure in the h9/14-*Alu* RNA complex as it is constrained by a U-turn at position U12 and by a sheared G11-G16 base pair. A similar structural motif is also found in the ribosomal RNA-protein complex of L11 (46,47). When base paired with loop L1.2, the three base pairs form a stack which is extended on both sides by a purine base from L2 and L1.2 (Fig. 1). The highly ordered structure of loop L2 may facilitate base pairing as well as the formation of the stack as four of the bases that participate belong to it. It is therefore feasible that in 2L1.2 and 3L1.2 SRPs, where loop L2 is unchanged, the constrained conformation of loop L2 facilitates formation of non-canonical base pairs with loop L1.2 by keeping its four bases in a stacked conformation. In contrast, mutations in loop L2 may change its conformation or simply disfavour stacking because purines have been replaced by pyrimidines. Loop L1.2 lacks internal stabilizing structures and its flexibility is consistent with non-canonical base pairing with loop L2. The finding that G13 was found to base pair with either C37 or U35 in the two *Alu* RNP structures illustrates its potential for alternative base pairing, although the G13-U35 base pair most likely represents an artefact caused by crystal contacts (20). Notably, the observation that 3L1.2 SRP has a slight defect in elongation arrest (Fig. 4) suggests that with an unchanged loop L2 structure, at least one Watson-Crick base pair is required for full activity of the tertiary structure. Another factor which might fortuitously influence the capacity to form alternative base pairs is that 2L1.2 and 3L1.2 RNAs have a majority of purine bases and 2L2 and 3L2 RNAs a majority of pyrimidine bases in their loops. The pyrimidines might be too distant to form hydrogen bonds whereas the purines may form non Watson-Crick base pairs.

The *Alu* domain of SRP RNAs of *Metazoa*, *Plantae* and *Archaea* as well as of the eubacterial species *Bacillus* and *Clostridium* (not shown) most likely all have the same overall fold as human *Alu* RNA, since the two helical stacks as well as the highly conserved U-turn motif linking the two stacks are preserved (Fig. 1 and 7). We have revised the previously published alignments (24) taking into consideration the conservation of essential structural nucleotides in the two hairpin structures of human *Alu* RNA (Fig. 7, (20)). As mentioned before, they include the base paired nucleotides (Fig. 7, red), the U-turn residue (star) and the sheared G-G base pair in loop L2 (green). The new alignment confirmed that all SRP RNAs of *Metazoa*, *Plantae* and *Archaea* can form tertiary base pairs between the two loops. In addition, the alignment reveals certain specific features for each group.

Metazoan SRP RNAs contain all the specific structural features of human *Alu* RNA, although some minor differences are observed. They include differences in the loop sizes of *D. melanogaster*

SRP RNA and an unusual U-U base pair preceding the sheared G-G pair in *X. laevis* SRP RNA. In plant SRP RNAs, loop L2 is highly conserved except that the U-turn residue is sometimes replaced by cytidine. This replacement may not have an important effect on the structure, since a C residue may introduce a U-turn-like bent as revealed by the pseudoknot structure of beet western yellow virus RNA (48). In certain cases, a non Watson-Crick base pair precedes the sheared G-G base pair. The most important difference is that the loop L1.2 is always smaller and helix 1.2 shorter by one base pair. However, sequence conservation and complementary nucleotide changes support formation of two base pairs between the loops. Furthermore, the two base pairs are adjacent to the G of the sheared base pair in loop L2 and the two base pairs and the adjacent G may therefore form a continuous stack as in human *Alu* RNA.

In SRP RNAs of *Archaea*, the U-turn residue is still conserved whereas the sheared G-G base pair is absent. Instead, there is often a G-U or A-U base pair lengthening helix H2. The base complementarities between the loops are clearly expanded to four nucleotides. The biggest changes are in helix 1.2 and loop L1.2. Only the first four base pairs are confirmed by sequence complementarities. They are followed by a highly conserved apparently single-stranded G residue. Its presence in all archaeal RNAs may highlight an important structural or functional role. The remaining nucleotides may either form a very large loop L1.2 (up to fifteen nucleotides) or extend helix H1.2 by non-canonical base pairing. As indicated in Fig. 7, an extension of H1.2 might be favoured, since large loops are thermodynamically unstable (49). The conserved G residue may allow bending of the longer helix thereby enabling loop L1.2 to base pair with L2 despite the presumably longer helix.

In summary, the conservation of the key structural features such as the constrained structure of loop L2 and the potential to form base pairs which may form an extended stack with bases from the loops L2 and L1.2 emphasises the importance of this tertiary structure for SRP functions. Notably, the tertiary structure is not conserved in SRP RNAs of *Protozoa* and *Fungi* (50-53), which have truncated *Alu*-like domains lacking one or both hairpin structures. In trypanosomes, the absence of the specific tertiary structure in the *Alu* domain might have been compensated for by the acquisition of an additional tRNA-like RNA in the SRP particle (31,32).

What is the function of the conserved tertiary structure in elongation arrest activity? The minor effects of the mutations on the dissociation constants of the complex are in agreement with binding of SRP9/14 to *Alu* RNA on the opposite side of the tertiary structure. In addition, the formation of the RNA binding surface of SRP9/14 (20) requires a largely intact protein complex and only very small changes in the C-terminal regions of SRP14 and SRP9 are tolerated without interfering with RNA binding (54). It is therefore unlikely that the structure of the SRP9/14 protein in the complex was changed significantly by the mutations in the RNA. As mentioned before, tertiary structure is most likely induced by protein binding (22) and it therefore contributes to the stability of the complex. The small changes in the dissociation constants and in the RNA binding efficiency are therefore plausibly explained by a slight diminished stability of the complex. It is also unlikely that the mutations in the two loops interfered with the formation of the closed complex. *Alu* RNA variants with mutations that interfere with the formation of the closed conformation have their dissociation constants reduced by 50-100-fold (25). In addition, the particles containing the mutated RNAs have intact signal recognition and targeting functions, arguing against a significant influence of the mutations on the overall structure of SRP. Although it cannot be excluded entirely, it is therefore rather unlikely that conformational changes in SRP9/14 or in the overall structure of SRP account for the observed effects of the mutations on elongation arrest activity.

A more attractive hypothesis is that the structure might be recognised by a ribosomal component. Indeed, the *Alu* domain is expected to make direct contacts with the ribosome to effect elongation arrest as deduced from the analysis of a truncated SRP14 protein. Interestingly, truncation of SRP14 has a more dramatic effect on elongation arrest activity of the particle than the disruption of the tertiary structure. Removal of only five amino acid residues (residues 96-100 in h14) at the C-terminus of SRP14 completely abrogates elongation arrest activity ((18,39), L.H. and K.S., unpublished results). Mutations in the two-loop structure do not completely abolish elongation arrest activity consistent with an auxiliary role of the tertiary structure, which may optimise the essential function of the C-terminal region in SRP14. This interpretation is supported by the result that increasing the concentration of the mutated particle 2L2 could compensate its defect in translocation efficiency. In addition, it may explain why certain organisms like *S. cerevisiae*, which contain SRP14

but apparently lack the tertiary structure, have an elongation arrest function (11). The interacting partner for the tertiary structure may be ribosomal RNA or protein. Ribosomal RNA may recognise the geometry of the base pairs as it has recently been observed in codon-anticodon recognition during translation (55) whereas a ribosomal protein may recognise the critical structure by shape. The results presented here clearly established an important role for the conserved tertiary structure in elongation arrest activity of SRP; future experiments will have to clarify its exact role in the mechanism of the elongation arrest function.

ACKNOWLEDGEMENTS

We would like to thank Dr. Gilles Moreau and Lionel Terzi for helpful and stimulating discussions, and Yiwei Miao and Yuanlong Shao for technical assistance. This work was supported by grants from the Swiss National Science Foundation, the Canton of Geneva and the MEDIC Foundation. S.C. and K.S. wish to acknowledge long-term support from the Swiss Government and the European Union Framework IV TMR programme for SRPNET (FMRX-CT960035) and Framework V Quality of Life programme for MEMPROT-NET (QLK3-CT200082). Support from NIH grant R01GM26494 and the Robert A. Welch Foundation are also acknowledged (A.E.J.).

REFERENCES

1. Keenan, R.J., Freymann, D.M., Stroud, R.M. and Walter, P. (2001) *Annual Review of Biochemistry*, **70**, 755-775.
2. Johnson, A.E. and van Waes, M.A. (1999) *Annu Rev Cell Dev Biol*, **15**, 799-842.
3. Rapoport, T.A., Jungnickel, B. and Kutay, U. (1996) *Annu. Rev. Biochem.*, **65**, 271-303.
4. Legate, K.R. and Andrews, D.W. (2001) *Biochem Cell Biol*, **79**, 593-601.
5. Walter, P., Ibrahimi, I., and Blobel G. (1981) *Journal of Cell Biology*, **91**, 545-550.
6. Hauser, S., Bacher, G., Dobberstein, B. and Lutcke, H. (1995) *Embo J.*, **14**, 5485-5493.
7. Flanagan, J.J., Chen, J.C., Miao, Y., Shao, Y., Lin, J., Bock, P.E. and Johnson, A.E. (2003) *J Biol Chem*, **278**, 18628-18637.
8. Ogg, S.C. and Walter, P. (1995) *Cell*, **81**, 1075-1084.
9. Walter, P. and Blobel, G. (1981) *J. Cell. Biol.*, **91**, 557-561.
10. Wolin, S.L. and Walter, P. (1989) *J Cell Biol*, **109**, 2617-2622.
11. Mason, N., Ciuffo, L.F. and Brown, J.D. (2000) *EMBO Journal*, **19**, 4164-4174.
12. Siegel, V. and Walter, P. (1985) *J Cell Biol*, **100**, 1913-1921.
13. Pool, M.R., Stumm, J., Fulga, T.A., Sinning, I. and Dobberstein, B. (2002) *Science*, **297**, 1345-1348.
14. Rinke-Appel, J., Osswald, M., von Knoblauch, K., Mueller, F., Brimacombe, R., Sergiev, P., Avdeeva, O., Bogdanov, A. and Dontsova, O. (2002) *Rna*, **8**, 612-625.
15. Gu, S.Q., Peske, F., Wieden, H.J., Rodnina, M.V. and Wintermeyer, W. (2003) *Rna*, **9**, 566-573.
16. Siegel, V. and Walter, P. (1988) *Cell*, **52**, 39-49.
17. Powers, T. and Walter, P. (1996) *Curr Biol*, **6**, 331-338.
18. Thomas, Y., Bui, N. and Strub, K. (1997) *Nucleic Acids Res*, **25**, 1920-1929.
19. Wild, K., Weichenrieder, O., Strub, K., Sinning, I. and Cusack, S. (2002) *Current Opinion in Structural Biology*, **12**, 72-80.
20. Weichenrieder, O., Wild, K., Strub, K. and Cusack, S. (2000) *Nature*, **408**, 167-173.
21. Strub, K., Moss, J. and Walter, P. (1991) *Mol Cell Biol*, **11**, 3949-3959.
22. Andreazzoli, M. and Gerbi, S.A. (1991) *Embo J*, **10**, 767-777.
23. Gorodkin, J., Knudsen, B., Zwieb, C. and Samuelsson, T. (2001) *Nucleic Acids Research*, **29**, 169-170.
24. Zwieb, C., Muller, F. and Larsen, N. (1996) *Fold. Des*, **1**, 315-324.
25. Weichenrieder, O., Stehlin, C., Kapp, U., Birse, D.E., Timmins, P.A., Strub, K. and Cusack, S. (2001) *Rna*, **7**, 731-740.
26. Weichenrieder, O., Kapp, U., Cusack, S. and Strub, K. (1997) *Rna*, **3**, 1262-1274.
27. Peluso, P., Herschlag, D., Nock, S., Freymann, D.M., Johnson, A.E. and Walter, P. (2000) *Science*, **288**, 1640-1643.
28. Peluso, P., Shan, S.O., Nock, S., Herschlag, D. and Walter, P. (2001) *Biochemistry*, **40**, 15224-15233.
29. Miller, J.D., Wilhelm, H., Gierasch, L., Gilmore, R. and Walter, P. (1993) *Nature*, **366**, 351-354.
30. Zheng, N. and Gierasch, L.M. (1997) *Mol Cell*, **1**, 79-87.
31. Beja, O., Ullu, E. and Michaeli, S. (1993) *Mol Biochem Parasitol*, **57**, 223-229.
32. Liu, L., Ben-Shlomo, H., Xu, Y.X., Stern, M.Z., Goncharov, I., Zhang, Y. and Michaeli, S. (2003) *J Biol Chem*, **278**, 18271-18280.
33. Arnaud, N., Cheynet, V., Oriol, G., Mandrand, B. and Mallet, F. (1997) *Gene*, **199**, 149-156.
34. Bovia, F., Wolff, N., Ryser, S. and Strub, K. (1997) *Nucleic Acids Res*, **25**, 318-326.
35. Studier, F.W., Rosenberg, A.H., Dunn, J.J. and Dubendorff, J.W. (1990) *Methods in Enzymology*, **185**, 60-89.
36. Strub, K. and Walter, P. (1990) *Mol Cell Biol*, **10**, 777-784.
37. Walter, P. and Blobel, G. (1983) *Methods Enzymol.*, **96**, 84-93.
38. Chang, D.Y., Newitt, J.A., Hsu, K., Bernstein, H.D. and Marais, R.J. (1997) *Nucleic Acids Res*, **25**, 1117-1122.
39. Bovia, F., Bui, N. and Strub, K. (1994) *Nucleic Acids Res.*, **22**, 2028-2035.

40. Janiak, F., Walter, P. and Johnson, A.E. (1992) *Biochemistry*, **31**, 5830-5840.
41. Walter, P. and Blobel, G. (1983) *Cell*, **34**, 525-533.
42. Walter, P. and Blobel, G. (1983) *Methods Enzymol.*, **96**, 682-691.
43. Kandels-Lewis, S. and Seraphin, B. (1993) *Science*, **262**, 2035-2039.
44. Vila-Sanjurjo, A. and Dahlberg, A.E. (2001) *J Mol Biol*, **308**, 457-463.
45. Noller, H.F., Green, R., Heilek, G., Hoffarth, V., Huttenhofer, A., Joseph, S., Lee, I., Lieberman, K., Mankin, A., Merryman, C. *et al.* (1995) *Biochem Cell Biol*, **73**, 997-1009.
46. Conn, G.L., Draper, D.E., Lattman, E.E. and Gittis, A.G. (1999) *Science*, **284**, 1171-1174.
47. Wimberly, B.T., Guymon, R., McCutcheon, J.P., White, S.W. and Ramakrishnan, V. (1999) *Cell*, **97**, 491-502.
48. Su, L., Chen, L., Egli, M., Berger, J.M. and Rich, A. (1999) *Nat Struct Biol*, **6**, 285-292.
49. Groebe, D.R. and Uhlenbeck, O.C. (1988) *Nucleic Acids Res*, **16**, 11725-11735.
50. Hann, B.C. and Walter, P. (1991) *Cell*, **67**, 131-144.
51. Michaeli, S., Podell, D., Agabian, N. and Ullu, E. (1992) *Mol Biochem Parasitol*, **51**, 55-64.
52. Ben-Shlomo, H., Levitan, A., Beja, O. and Michaeli, S. (1997) *Nucleic Acids Res*, **25**, 4977-4984.
53. Strub, K., Fornallaz, M. and Bui, N. (1999) *Rna.*, **5**, 1333-1347.
54. Bui, N., Wolff, N., Cusack, S. and Strub, K. (1997) *RNA*, **3**, 748-763.
55. Ogle, J.M., Brodersen, D.E., Clemons, W.M., Jr., Tarry, M.J., Carter, A.P. and Ramakrishnan, V. (2001) *Science*, **292**, 897-902.

Figure legend

Figure 1: Structure of the SRP *Alu* domain. **(A)** Secondary structure of the synthetic SRP RNA *Alu* domain. Stems and loops are named according to the topological nomenclature. Bases in the loops, which form tertiary base pairs are highlighted in red. Protein and RNA footprints are shown in bold. Stretches of ten nucleotides are marked in blue. **(B)** Structure model of the SRP *Alu* domain as derived from two crystal structures. SRP9 and SRP14 are displayed as red and green ribbons respectively. Nucleotides from loops L2 and L1.2 that are involved in tertiary interactions between the loops are shown as wireframe. The protein makes contacts to the U-turn as well as to the central stem. **(C)** Detailed view of the tertiary base pairing between loops L2 and L1.2. Bases G13, G14 and C15 form hydrogen bonds with C37, C34 and G33, respectively (dotted green lines). One base from each loop, G16 and A36, are positioned to extend the stack formed by the three base pairs.

Figure 2: Binding of human SRP9/14 to mutated SRP RNAs. **(A)** Description and names of the mutated SRP RNAs. L2 and L1.2 mutations disrupt base pairing whereas Comp mutations restore base pairing with a different sequence. **(B)** *In vitro* synthesized [³⁵S]-labelled h14 combined with recombinant h9 were bound to biotinylated mutated SRP RNAs as indicated on top of each lane. The RNA-bound proteins were submitted to SDS-PAGE followed by autoradiography. The input represents 1/3 of the total [³⁵S]-labelled h14 protein used in the experiments. Neg: as a negative control we used rat 4.5S RNA. Lower panel h9/14 binding was quantified by phosphorescence imaging. **(C)** Protein binding efficiencies of mutated SRP RNAs in which guanidines and cytidines were replaced by adenines and uridines. The binding efficiencies of the mutated RNAs were normalised to wild type RNA (WT), which was set to 100%.

Figure 3: Apparent dissociation constants of mutated SA86 *Alu* RNAs. **(A)** The h9/14-SA86 complex and free SA86 were separated on 8% native RNA gel. Increasing amounts of 3 Comp *Alu* RNA was added as a competitor. WT alone: SA86 *Alu* RNA. WT+BSA: h9/14 was replaced with the same amount of bovine serum albumin. WT+h9/14: Complex formation in the absence of competitor RNA. **(B)** Complex formation was quantified by phosphorescence imaging and the apparent ratio of the dissociation constants calculated as described in Material and Methods. WT: SA86 *Alu* RNA. 2L2, 2L1.2, 2 Comp and 3 Comp: The same mutations as described in Fig. 2A in the SA86 *Alu* RNA. K_{dc} and K_{dwt} : Dissociation constants of the mutated and of SA86 *Alu* RNAs, respectively.

Figure 4: Elongation arrest and translocation activities of particles reconstituted with mutated SRP RNAs. **(A)** An example of elongation arrest and translocation assays. SRPs were reconstituted with canine and recombinant proteins and with canine, synthetic and mutated synthetic SRP RNAs. Reconstituted SRPs were added at a final concentration of 100 nM to 10 μ l wheat germ translation reactions programmed with sea urchin cyclin and bovine preprolactin mRNAs. SRP-depleted microsomes were added to assay translocation activities. After 30 min the reaction was stopped and the samples analysed by SDS-PAGE. Upper panel: Elongation arrest assays; lower panel: Translocation assays. Neg. : Negative control, reconstitution in the absence of h9/14; lanes 3-7: Particles reconstituted with SRP RNAs: cSRP: Canine SRP RNA; WT : Synthetic SRP RNA. **(B)** Quantification of the elongation arrest activities of mutated SRPs. The relative inhibition in the accumulation of preprolactin as compared to cyclin was calculated for each sample. The ratio of preprolactin to cyclin in the negative control was taken as 0% inhibition. **(C)** Quantification of the translocation activities of SRP. Values represent the ratio between prolactin and the total amount of preprolactin synthesised (preprolactin and prolactin). WT: Particles reconstituted with WT SRP RNA. Values represent the average of two or more independent experiments.

Figure 5: Effects of increasing RNA and h9/14 concentrations on the activities of 3L2 SRP. **(A)** Elongation arrest assays of particles reconstituted with increasing amounts of 3L2 and, as a positive control, with WT SRP RNAs. 0.5x, 1X, 1.5x, 2x, 4x, 8x indicates the ratio between RNA and proteins.

White bars: WT RNA; grey bars: 3L2 RNA. **(B)** Translocation assays with 3L2 SRP. S: standard reconstitution with WT SRP RNA standardised to 100 %. **(C)** Elongation arrest assays of 3L2 particles reconstituted with increasing amounts of h9/14. WT: Reconstitution with WT SRP RNA; 1x: Standard reconstitution of 3L2 particles; 2x, 4x, 8x: Excess of h9/14 as compared to 1x. **(D)** Translocation assays with the same particles as in C. Values represent the average of two or more independent experiments.

Figure 6: Elongation arrest and translocation activities of purified SRPs. **(A)** Purification of WT SRP by DE53 chromatography. Column fractions analysed by 5-20% SDS-PAGE and silver nitrate staining. FT: flow through, W: wash, lanes 1 and 2: elutions at 600 mM KOAc, lanes 3 and 4: elutions at 1M KOAc. Fully reconstituted SRP is in lane 1. **(B)** Comparison of the different reconstituted particles after purification. Lane 1: WT; lane 2: 2L2; Lane 3: 2 Comp. The concentrations of the different SRPs were subsequently determined by Western blotting. **(C and D)** Elongation arrest and translocation activities are plotted against the concentration of purified SRP used in the assay. WT: black line, 2L2: dotted line, 2 Comp: dashed line. Values represent the average of at least four independent experiments. At low elongation arrest activities, the error bars were reproducibly more elevated.

Figure 7: Evolutionary conservation of the tertiary structure. **(A)** Loop L1.2 and loop L2 sequence alignments of a representative sample of metazoan, plant and archaeal species. Loop sequences are labelled with a black bar and the adjacent helix sequences are outlined in bold italic, dotted line: borders of loop sequences not unambiguously identified. **(B)** Secondary structure models of the 5' *Alu* domain. Green: sheared G-G base pair, red: base paired nucleotides in the loops, blue: conserved nucleotide in *Archaea*.

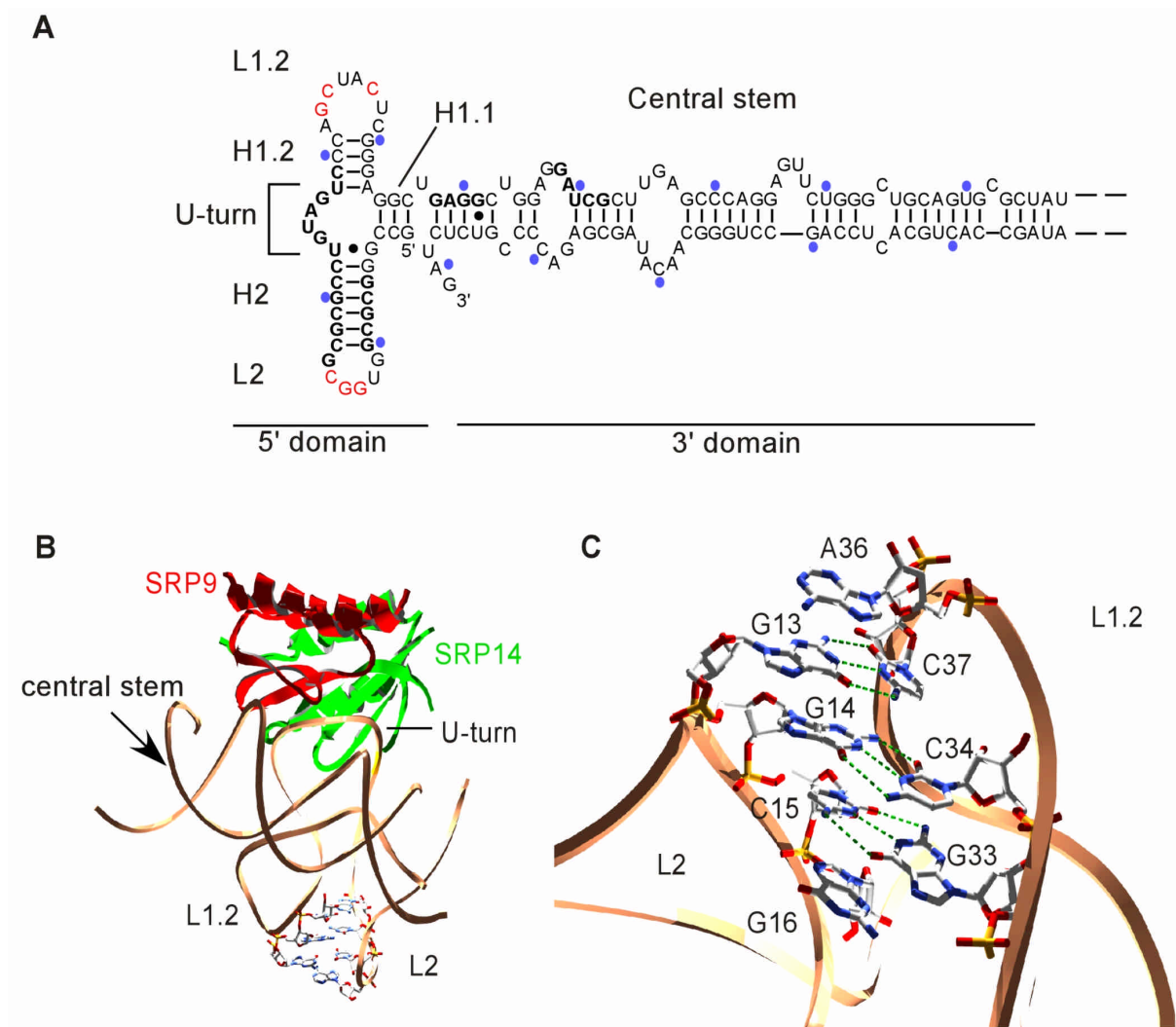
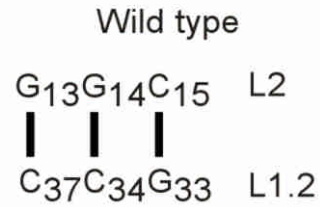
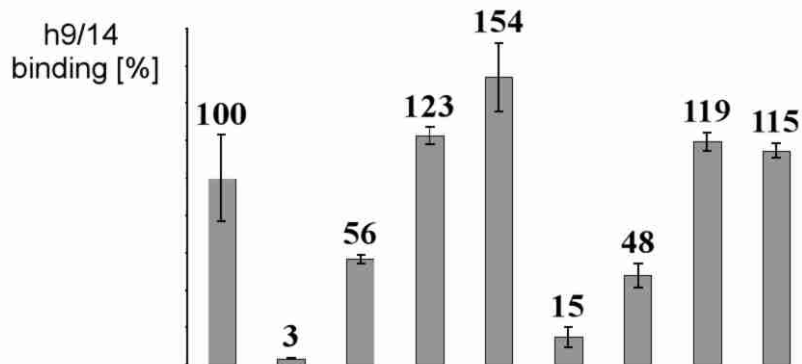
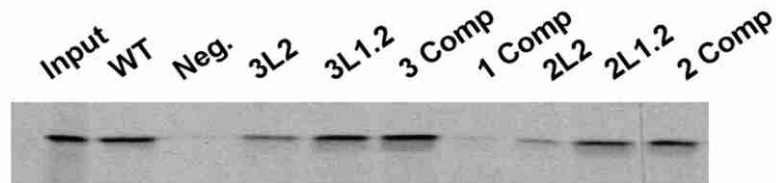


Figure 1

A

Name	2L2	3L2
Mutations	C ₁₃ C ₁₄	C ₁₃ C ₁₄ G ₁₅
Name	2L1.2	3L1.2
Mutations	G ₃₇ G ₃₄	G ₃₇ G ₃₄ C ₃₃
Name	2 Comp	3 Comp
Mutations	C ₁₃ C ₁₄ G ₃₇ G ₃₄	C ₁₃ C ₁₄ G ₁₅ G ₃₇ G ₃₄ C ₃₃

**B****C**

Mutations	U ₁₄ U ₁₅	A ₃₃ A ₃₄	U ₁₄ U ₁₅ A ₃₃ A ₃₄
h9/14 binding [%]	41 ± 4	111 ± 25	117 ± 23
Mutations	A ₁₄ A ₁₅	U ₃₃ U ₃₄	A ₁₄ A ₁₅ U ₃₃ U ₃₄
h9/14 binding [%]	44 ± 13	77 ± 3	97 ± 12

Figure 2

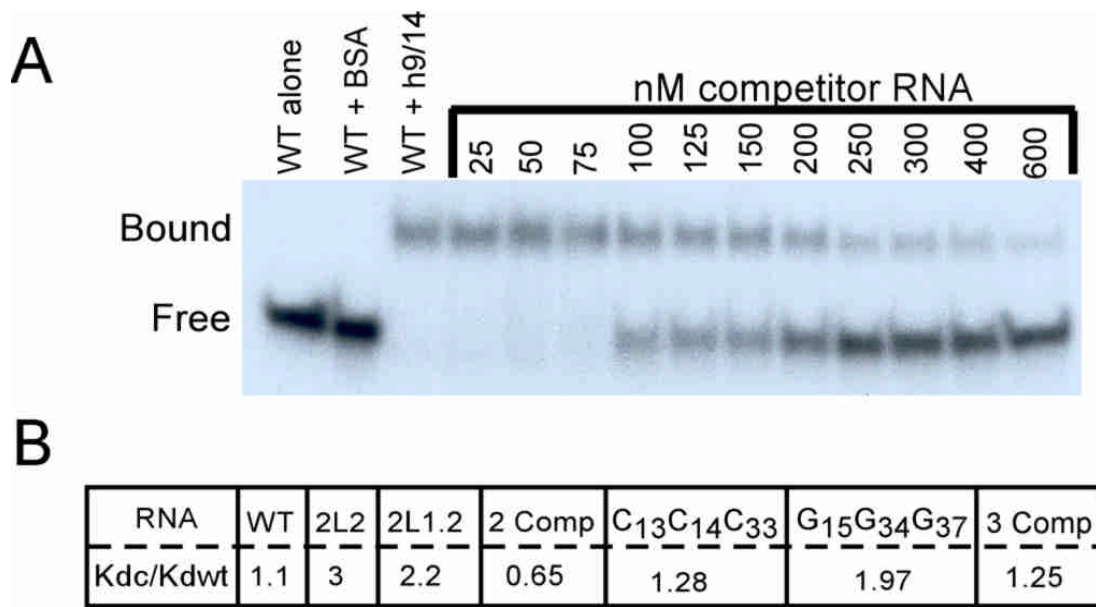


Figure 3

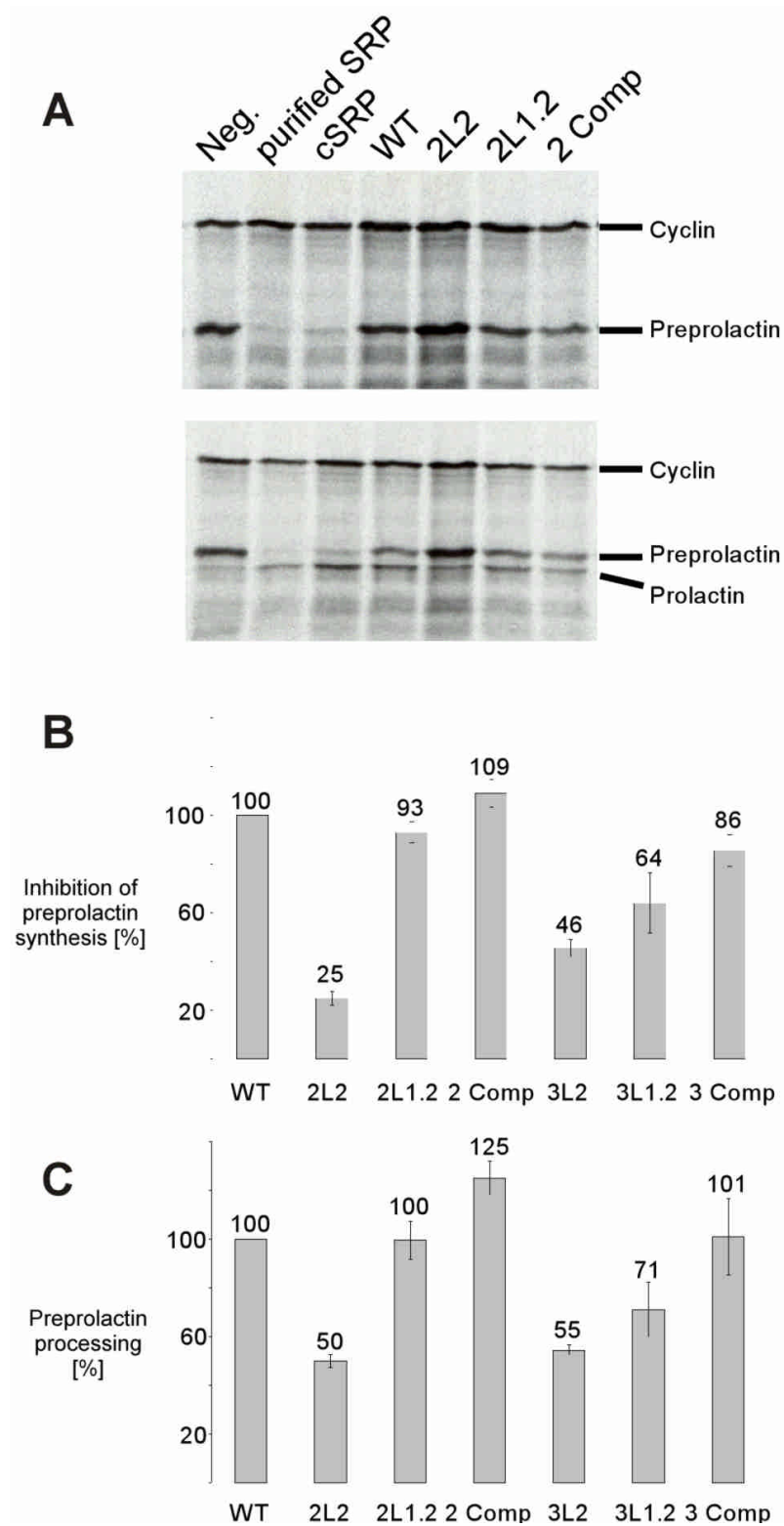


Figure 4

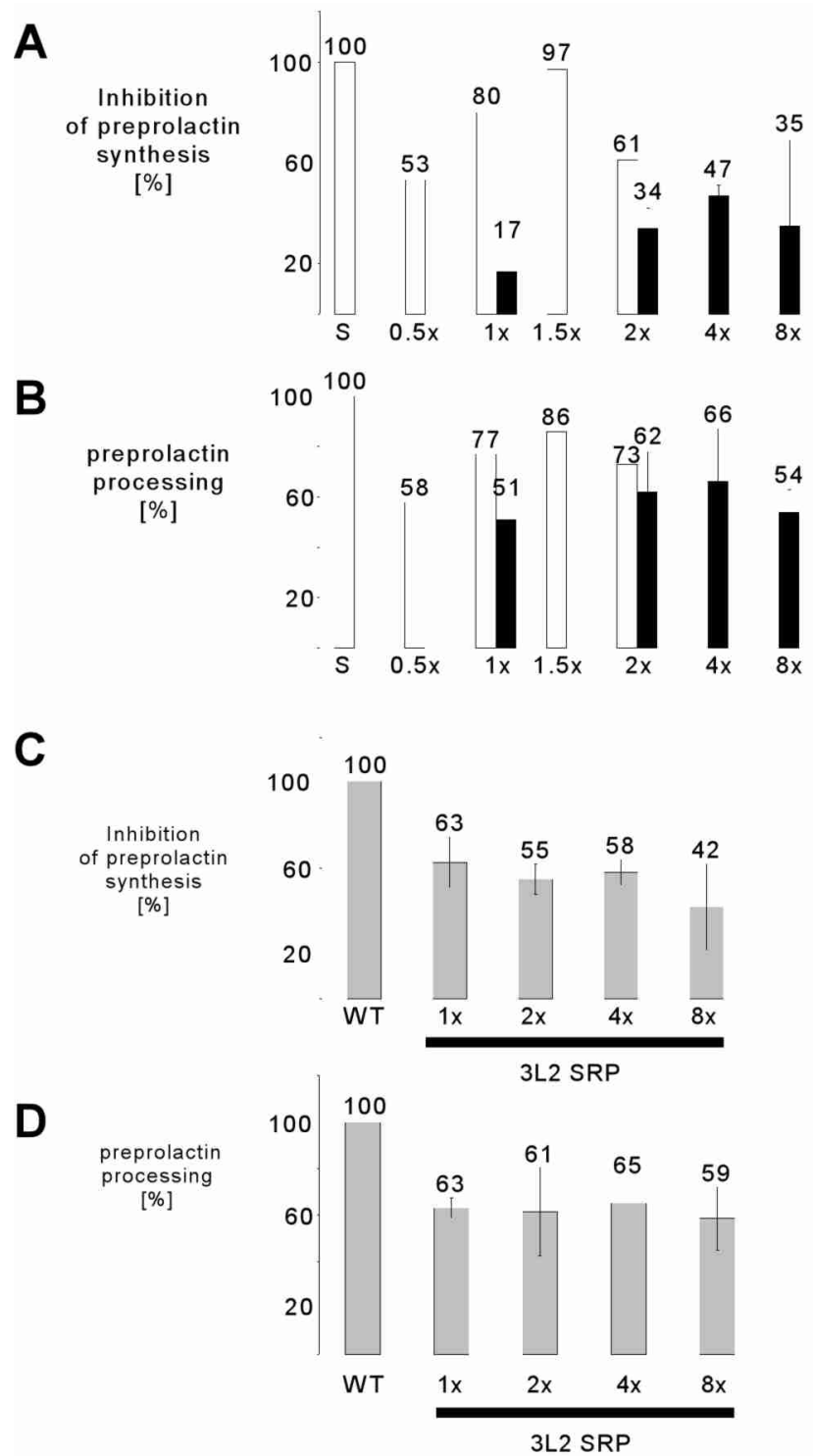


Figure 5

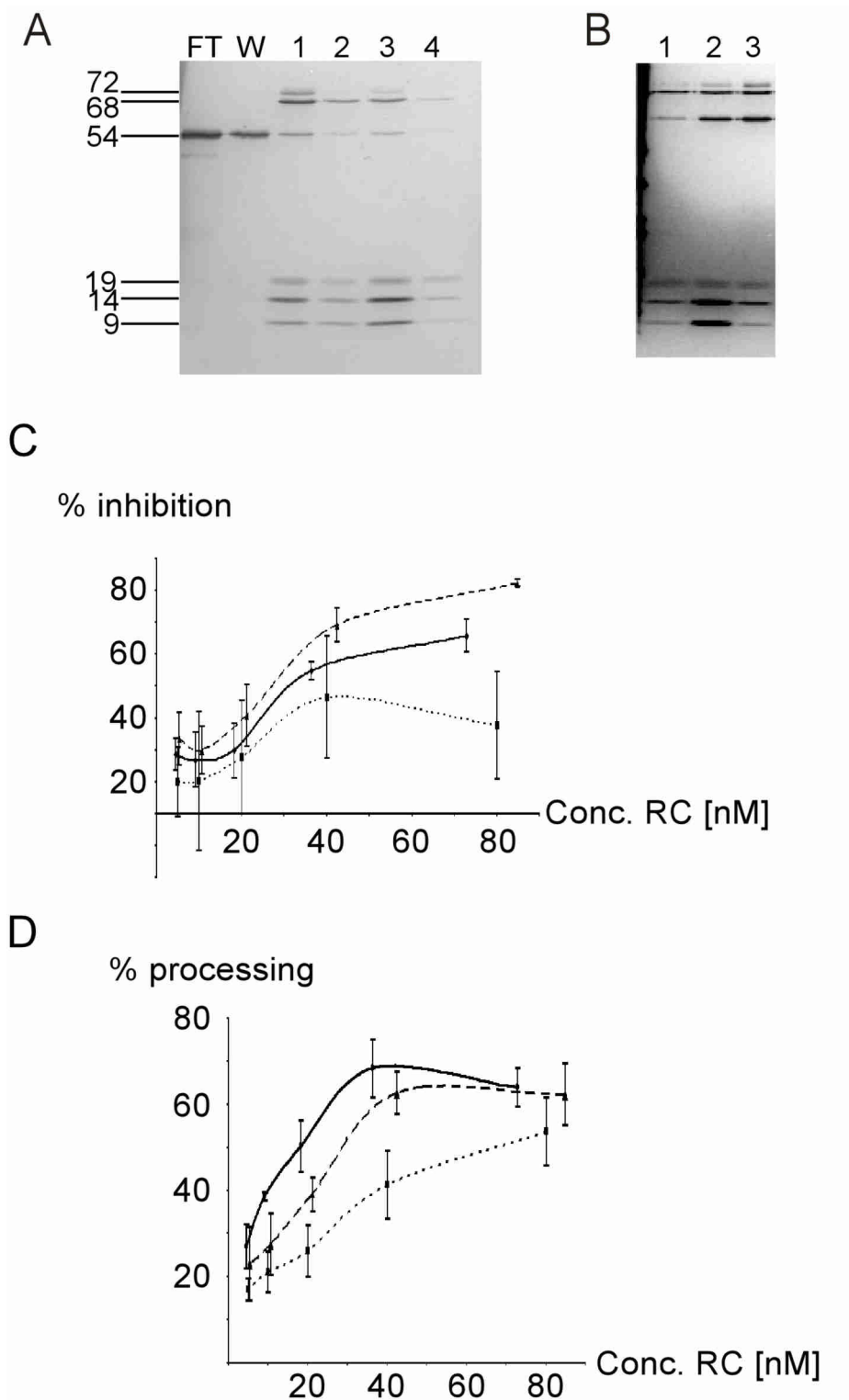


Figure 6

A

		Loop L2		Loop L1.2	
METAZOA	H. sapiens	G	G U G G C G C	C A G C U A C U C G	
	C. species	G	G U G G C G C	C A G C U A C U C G	
	M. musculus	G	G U G G C G C	C A G C U A C U C G	
	X.laevis	U	G U G G C G U	C A G C U A C U U G	
	D. melanogaster	G	G U U G G C A G C	C G C U U C U G	
	C. elegans	C	G U G G C G G	A G C U U C U U	
PLANTAE	Z. mays	C U	G U A G C G A G	C G A G C G	
	T. aestivum	C A	G U U G C G A G	C G A G U G	
	A. thaliana	A A	G U A A C A A U	C A U G U G	
	H. japonicus	U A	G C A A C G U G	C A A G U G	
	H. lupulus	U A	G C A A C G U G	C A A G U G	
	L. esculentum	U A	G U A A C G U G	C A A G U G	
	B. hispida	C A	G C A G U G U G	C G A A C G	
ARCHAEA	H. halobium	G U U	U G G C U C	G U G A G A C A G U C A U C A G C	
	M. jannaschii	G U U	G G G C G U	G A A A U C G C C C U U A U G C	
	P. horikoschii	G U U	C G G C G U	G A A A C C G C C G A U A U G C	
	S. sulfataricus	U C U	C G C C A G	A C A U G G C G C A A C G U	
	T. celer	G U U	C G G C G U	G A A A C C G U C G A U A C G C	

B

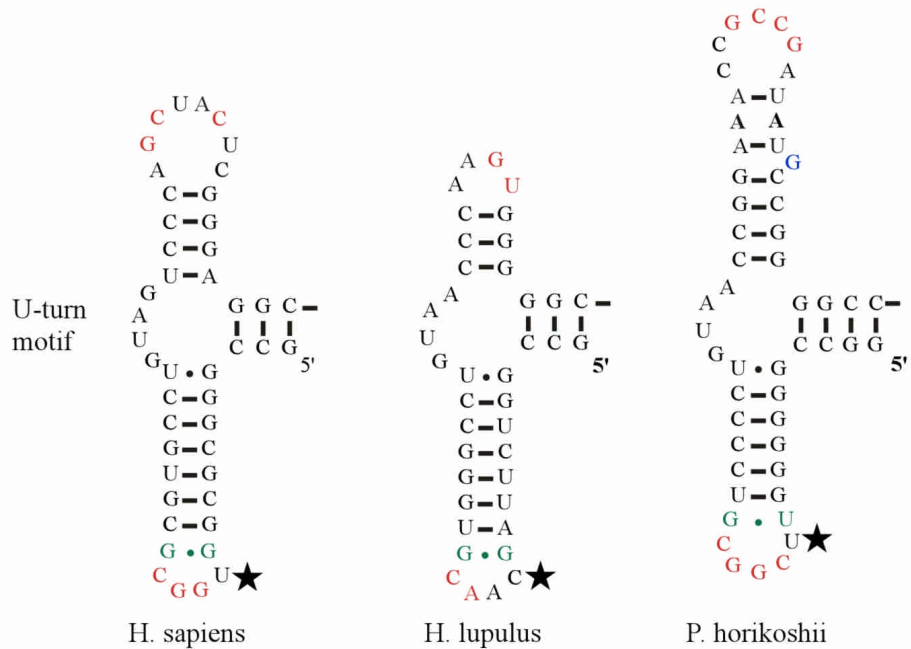


Figure 7